# Theoretical Study of the Stereoselective Additions of Chiral Alcohols to Ketenes

Carina E. Cannizzaro and K. N. Houk*

*Contribution from the Department of Chemistry and Biochemistry, University of California, Los Angeles, California 90095-1569*

Received May 1, 2003; E-mail: houk@chem.ucla.edu

***Abstract:*** In 1989, Larsen et al. at Merck discovered that the addition of chiral alcohols to ketenes provided enantiomerically enriched aryl propionic acids, compounds valued for their therapeutic antiinflammatory properties. The high 1,4-asymmetric induction observed (>99:1 dr in the addition, and up to 99% ee after hydrolysis to the acid) is rare. A quantitative model based on B3LYP density functional theory calculations accounts for the stereoselectivity in the addition of (*S*)-methyl lactate, (*S*)-3-methyl-2-butanol, and (*S*)-pantolactone to methylphenylketene. The conformational processes of the intermediates can impact the stereoselectivity of the process, and either the addition step, or the protonation of the enolate intermediate, may be stereoselectivity determining.

## Introduction

Diastereoselective additions of chiral alcohols to ketenes have been known since 1919,[1,2] but a particularly useful class of reactions of this type was discovered by Larsen et al. at Merck in 1989.[1a] As shown in Scheme 1, the reactions of α-hydroxy esters and lactones with aryl alkyl ketenes proceed with high stereoselectivity. The products can be hydrolyzed to give optically active nonsteroidal antiinflammatory drugs.

The therapeutic efficacy of this class of drugs is shown by the extensive use of more than a dozen compounds exemplified by Ibuprofen, Naproxen, Ketoprofen, Flurbiprofen, and Flunoprofen shown in Figure 1.[2,5a] The awareness of the higher activity of the (*S*)-enantiomer of Ibuprofen and Naproxen[3] led to synthetic efforts[4] to obtain these acids enantiomerically pure.

The high 1,4-asymmetric induction observed (>99:1 dr; up to 99% ee) is rare,[5] and no mechanism that rationalizes the direction or magnitude of the stereoselectivity was proposed until 2001. At that time, we explored the reaction of methyl lactate with methylphenylketene with quantum mechanical calculations. In a preliminary communication,[6] we provided a quantitative model that accounts for the origin of stereoselectivity. We have now explored additional examples and provide a more complete interpretation of the experimental observations.
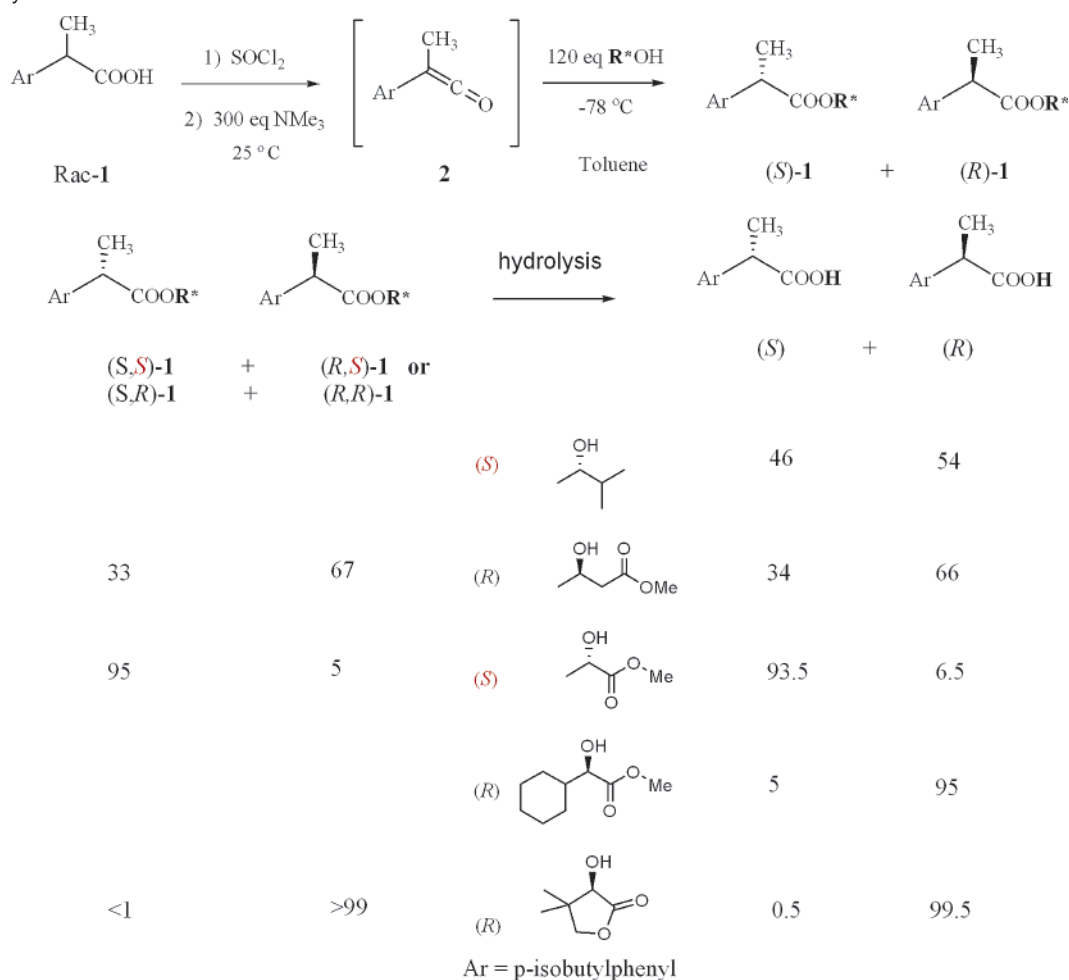
## Experimental Background

Several mechanisms have been proposed for the addition of alcohols to ketenes in the absence of base.[8-11] These include cyclic transition states for direct addition to the alkene[7-9] and acyclic transition states for initial addition to the carbonyl group.[1b,10]

On the basis of kinetic studies and the observation that the reaction rate is not enhanced by increasing polarity of the solvent, different groups proposed that the addition of alcohols to ketenes occurs via cyclic transition states containing one,[8] two,[9] or three[10] alcohol molecules. Figure 2 shows these transition states for the concerted addition of alcohol to ketene. Depending on the temperature, the reaction rates are first order, **4**, second order, **5**, or third order, **6**, in alcohol concentration.

An alternative mechanism for the reaction of 1-phenylethanol with methylphenylketene has been provided by Jähme and Ruchardt[1b] based on the effects on reactivity of changes in concentration, temperature, the structure of alcohol, and deu-

(1) (a) Anders, E.; Ruch, E. *Angew. Chem., Int. Ed. Engl.* **1973**, *12*, 25−29. (b) Jähme, J.; Rüchardt, C. *Angew. Chem., Int. Ed. Engl.* **1981**, *20*, 885. (c) Salz, U.; Rüchardt, C. *Tetrahedron Lett.* **1982**, *23*, 4017−4020. (d) Bellucci, G.; Berti, G.; Bianchini, R.; Vecchiani, S. *Gazz. Chim. Ital.* **1988**, *118*, 451. (e) Buschmann, H.; Scharf, H.-D.; Hoffmann, N.; Esser, P. *Angew. Chem.* **1991**, *103*, 490. (f) Fehr, C. *Angew. Chem.* **1996**, *108*, 2726. (g) Donohoe, G.; Satchell, D. P. N.; Satchell, R. S. *J. Chem. Soc., Perkin Trans. 2* **1990**, 1671. (h) Hodous, B. L.; Ruble, J. C.; Fu, G. C. *J. Am. Chem. Soc.* **1999**, *121*, 2637−2638.
(2) (a) Larsen, R. D.; Corley, E. G.; Davis, P.; Reider, P. J.; Grabowski, E. J. J. *J. Am. Chem. Soc.* **1989**, *111*, 7650. (b) Calmes, M.; Daunis, J.; Jacquier, R.; Natt, F. *Tetrahedron* **1994**, *50*, 6875−6880. (c) Camps, P.; Gimenez, S. *Tetrahedron: Asymmetry* **1995**, *6*, 991−1000. (d) Calmes, M.; Daunis, J.; Mai, N.; Natt, F. *Tetrahedron Lett.* **1996**, *37*, 379−380. (e) Calmes, M.; Daunis, J.; Mai, N.; Natt, F. *Tetrahedron* **1997**, *53*, 13719−13726. (f) Calmes, M.; Daunis, J.; Mai, N. *Tetrahedron: Asymmetry* **1997**, *8*, 1641−1648.
(3) Rieu, J.-P.; Boucherle, A.; Cousse, H.; Mouzin, G. *Tetrahedron* **1986**, *42*, 4095−4131.
(4) Shen, T. Y. *Angew. Chem., Int. Ed. Engl.* **1972**, *6*, 460.

(5) For a review: (a) Sonawane, H. R.; Bellur, N. S.; Ahuja, J. R.; Kulkarni, D. G. *Tetrahedron: Asymmetry* **1992**, *3*, 163−192. (b) Zhao, H.; Wu, Y. L. *Chin. Chem. Lett.* **1994**, *5*, 461−464. (c) Wan, K. T.; Davis, M. E. *J. Catal.* **1994**, *148*, 1−8. (d) Wan, K. T.; Davis, M. E. *J. Catal.* **1995**, *152*, 25−30. (e) Griesbach, R. C.; Hamon, D. P. G.; Kennedy, R. J. *Tetrahedron: Asymmetry* **1997**, *8*, 507−510. (f) Ishibashi, H.; Maeki, M.; Yagi, J.; Ohba, M.; Kanai, T. *Tetrahedron* **1999**, *55*, 6075. (g) Rajanbabu, T. V. *Chim. Oggi* **2000**, *18*, 26−31.
(6) The 1,4-asymmetric induction in enamine alkylations has previously been described theoretically: Lucero, M. J.; Houk, K. N. *J. Am. Chem. Soc.* **1997**, *119*, 826.
(7) Cannizzaro, C. E.; Strassner, T.; Houk, K. N. *J. Am. Chem. Soc.* **2001**, *123*, 1668−1669.
(8) Brady, W. T.; Vaughn, W. L.; Hoff, E. F. *J. Org. Chem.* **1969**, *34*, 843−845.
(9) Tille, A.; Pracejus, H. *Chem. Ber.* **1967**, *100*, 196−210.
(10) Lillford, P. J.; Satchell, D. P. N. *J. Chem. Soc. B* **1968**, 889−897.
(11) Jähme, J.; Rüchardt, C. *Tetrahedron Lett.* **1982**, *23*, 4011−4014.

**Scheme 1.** Asymmetric Addition of Chiral Alcohols to Ketenes[2a] [a]



| | | | | | |
|---|---|---|---|---|---|
| | 33 | 67 | (R) | 34 | 66 |
| | 95 | 5 | (S) | 93.5 | 6.5 |
| | | | (R) | 5 | 95 |
| | <1 | >99 | (R) | 0.5 | 99.5 |

Ar = p-isobutylphenyl

[a] The numbers shown correspond to diastereomer ratios obtained before hydrolysis on the left, and enantiomeric ratios obtained after hydrolysis on the right.
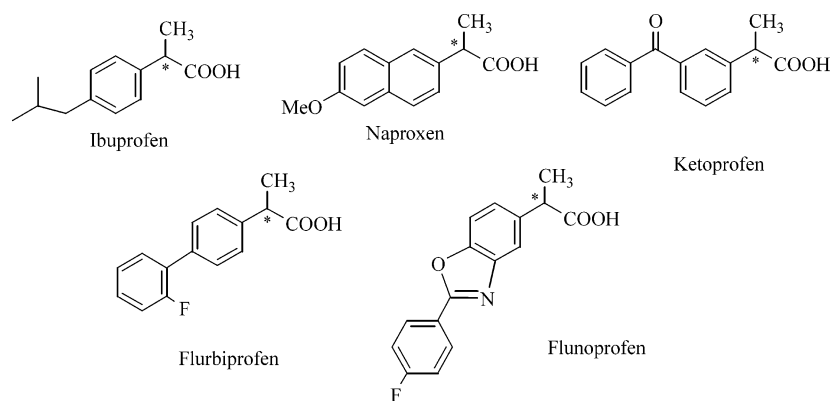


**Figure 1.** Commonly used NSAIDs.

terium isotope effects.[11] They observed an inverse dependence of rate on temperature, small or even negative activation enthalpies, and very large negative entropies of activation. Figure 3 shows the postulated mechanism that consists of a fast reversible addition of the first alcohol molecule to the ketene carbonyl to give small amounts of an intermediate zwitterion **7** or an enol **8**, followed by tautomerization to the keto form catalyzed by the second alcohol molecule in the rate-limiting step.

The reactions between trifluoromethylphenylketene and a series of chiral secondary alcohols gave diastereomeric esters

in ratios that ranged from 50% to 68%.[1a] Greater diastereoisomeric excesses correlated with larger differences in size between
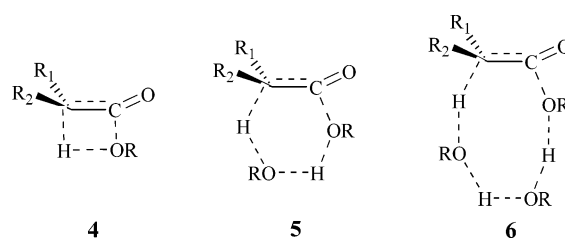


**Figure 2.** Cyclic transition states for the addition of alcohols to ketenes.
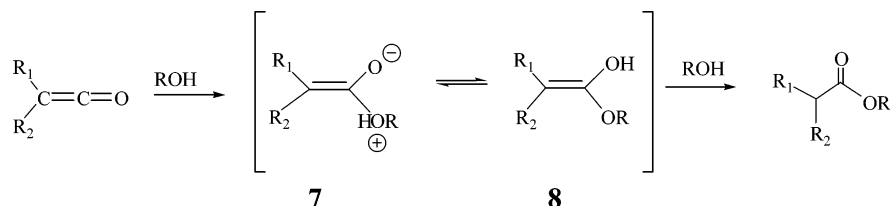
**Figure 3.** The Jähme and Rüchardt mechanism for the addition of 1-arylethanols to arylmethylketenes.
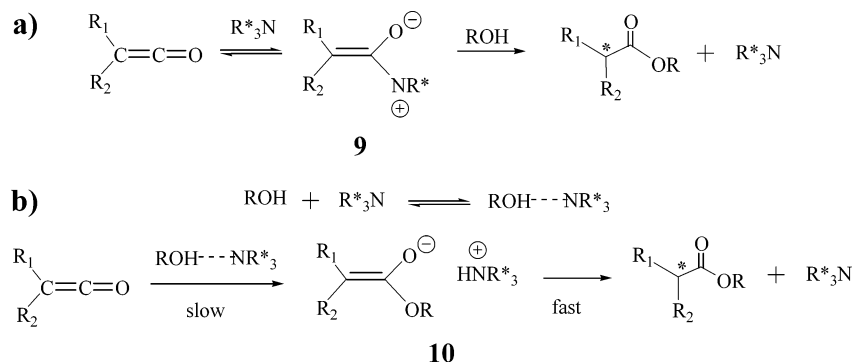


**Figure 4.** Possible mechanisms for the addition of alcohols to ketenes catalyzed by chiral tertiary amines.

**Table 1.** Calculated Activation Energies for the Dehydration of Acetic Acid

| investigator (ref) | geometry method | energy method | activation energy[b] |
|---|---|---|---|
| | One-Step Mechanism | | |
| Ruelle (14d) | HF/6-31G | MP4/6-31G | 78.4 |
| Skancke (14a) | HF/6-31G* | MP4/6-31G | 81.3 |
| Page (14a) | MCSCF[a]/6-31G* | G2 | 76.4 |
| this work | Becke3LYP/6-31G* | Becke3LYP/6-31G* | 85.6 |
| | Two-Step Mechanism | | |
| Xie (14c) | HF/3-21G | MP4(SDQ)/3-21G | 83.0 |
| Skancke (14a) | HF/6-31G* | MP4/6-31G* | 80.6 |
| Page (14b) | MCSCF[a]/6-31G* | G2 | 73.1 |
| this work | Becke3LYP/6-31G* | Becke3LYP/6-31G* | 74.4 |
| single-pulse shock tube measurements (6) | | | 67.5–72.7 |

[a] Complete active space MCSCF with a 10-electron, 10-orbital active space. [b] Energies in kcal/mol relative to acetic acid and corrected for zero-point vibrational energy differences.

the two groups in the secondary alcohol. The presence of achiral bases such as pyridine and 1,4-diazabicyclo[2.2.2]octane greatly enhanced the observed stereoselectivity.[1c,11]

The addition of methanol to methylphenylketene catalyzed by chiral tertiary amines (chinchona alkaloids) was extensively studied by Pracejus and co-workers.[9,11] Two possible mechanisms were considered to account for the effect of temperature, base, and solvent on the reaction rate, as well as the kinetic isotope effect observed upon substitution of MeOH by MeOD. Figure 4 shows the two different mechanisms: (a) nucleophilic attack of amine on the ketene carbonyl to give zwitterion **9**, or (b) base-catalyzed addition of alcohol to the ketene carbonyl to give the ion-pair **10**. The mechanism favored by Pracejus, (b), involves the initial formation of an amine alcohol complex, which reacts with methylphenylketene in the rate-determining step of the reaction to give the ion-pair intermediate which collapses to product.

Recently, Fu and co-workers postulated a mechanism similar to the one shown in Figure 4a as a working hypothesis for the enantioselective addition of MeOH to methylphenylketene catalyzed by a planar-chiral azaferrocene.[1h]
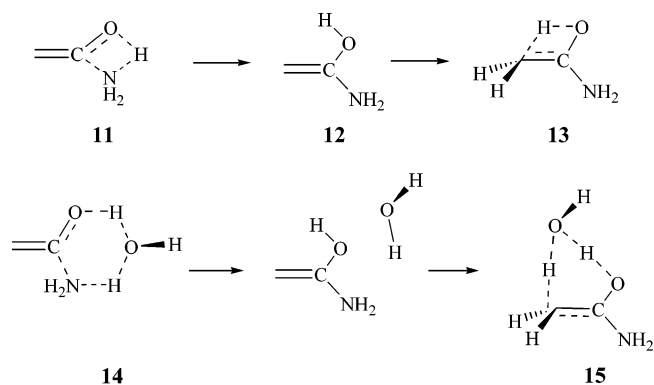


**Figure 5.** Addition of ammonia to ketene.

## Theoretical Background

There have been a variety of previous computational studies of nucleophilic additions to ketenes.[12] The most relevant are the studies on ketene hydration[13] that considered two possible mechanisms, a concerted addition of water to the C=C of the ketene, and a two-step process that involved initial addition of water to the ketene carbonyl followed by tautomerization to the acid. The energies of activation calculated using different methods are summarized in Table 1. The computed DFT results from the two-step mechanism reproduced closely the experimental energy of activation.[14]

The reactants, transition states, and intermediates for the addition of water to ketene were calculated at the B3LYP/6-31G* level of theory and compared to the results obtained using the highly accurate G2[15] method (Scheme 2) on fully optimized

(12) (a) Pracejus, H. *Justus Liebigs Ann. Chem.* **1960**, *634*, 9–22. (b) Pracejus, H.; Mätie, H. *J. Prakt. Chem.* **1964**, *24*, 195–205. (c) Samtleben, R.; Pracejus, H. *J. Prakt. Chem.* **1972**, *314*, 157–169. (d) Pracejus, H.; Leska, J. *Naturforsch.* **1966**, *21B*, 30–32. (e) Pracejus, H. *Fortschr. Chem. Forsch.* **1967**, *8*, 493–553.

(13) (a) Raspoet, G.; Nguyen, M. T.; Kelly, S.; Hegarty, A. F. *J. Org. Chem.* **1998**, *63*, 9669–9677. (b) Raspoet, G.; Nguyen, M. T.; McGarraghy, M.; Hegarty, A. F. *J. Org. Chem.* **1998**, *63*, 6878–6885. (c) Raspoet, G.; Nguyen, M. T.; McGarraghy, M.; Hegarty, A. F. *J. Org. Chem.* **1998**, *63*, 6867–6877. (d) Nguyen, M. T.; Raspoet, G.; Vanquickenborne, L. G. *J. Chem. Soc., Perkin Trans. 2* **1999**, 813–820. (e) Fang, D.-C.; Fu, X.-Y. *Theochem-J. Mol. Struct.* **1998**, *455*, 59–68.

**Scheme 2.** Model Calculations for the Addition of Water to Ketene at the B3LYP/6-31G* Level[a]



● Becke3LYP/6-31G*//Becke3LYP/6-31G*

● G2//MCSCF/6-31G*
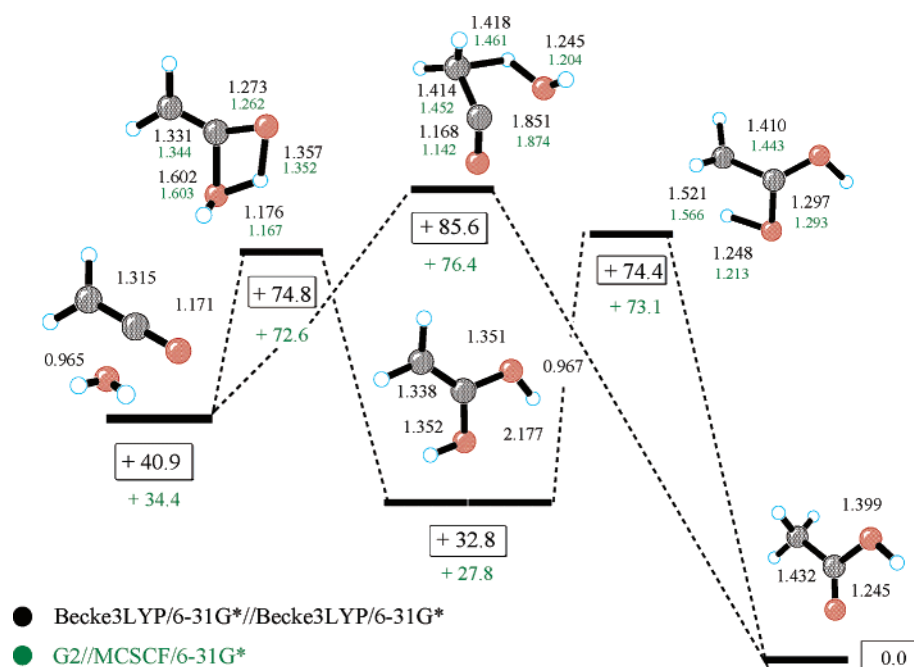
[a] Relative energies are in kcal/mol.

structures at the MP2 level. Both sets of calculations are consistent with a two-step mechanism in which the water adds to the ketene carbonyl with concomitant proton transfer to give an enol intermediate that subsequently tautomerizes to product.

B3LYP overestimates the $E_a$ for the one-step mechanism, as compared to G2 calculations. For the preferred mechanism, on the other hand, the B3LYP fully optimized structures are close to those obtained with the MCSCF method ($\pm 0.01-0.03$ Å), and this better agreement translates into comparable energy differences. The reasonable performance of the B3LYP/6-31G* level validates its use for the study of larger systems at a much lower computational cost.
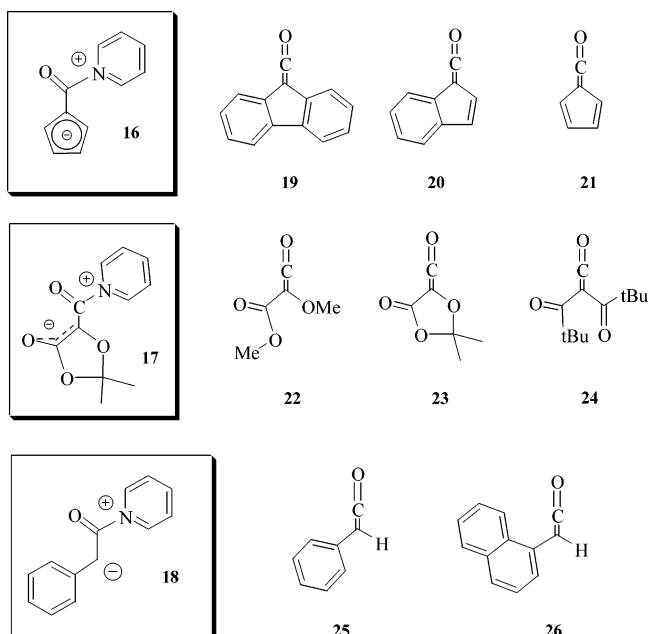


**Figure 6.** Ketenes that give stable ketene−pyridine zwitterionic adducts.

Theoretical studies on the amination of ketenes (Figure 5) have shown that no stable zwitterionic structures were located either in the gas phase or in polar solvent continuum for the addition of $NH_3$ to ketene.[16] The rate-determining step corresponded to a cyclic transition state for addition across the carbonyl of the ketene, **11**, to give an enol amide intermediate, **12**, that tautomerizes to the amide product in a subsequent, lower energy step, **13**. A water molecule was shown to catalyze the addition of ammonia to the C=O by acting as a hydrogen bond donor toward the ketene carbonyl and as a hydrogen bond acceptor toward ammonia, **14**.[16,17] It also lowered the energy of the tautomerization step by assisting the 1,3-H shift from the enolate oxygen to the carbon, **15**.

Inclusion of solvent (cavity model with dielectric constant: $\epsilon = 78.3$) did not change significantly the energetic profile of the reaction.[16] The large preference for the two-step reaction path across the C=O of ketene over the concerted mechanism involving addition across the C=C is maintained irrespective of the reaction conditions (in the gas phase or in solution, with or without a catalytic water molecule). Kinetic studies supported the formation of enol amides as intermediates when primary and secondary amines were used.[16] However, tertiary amines greatly reduce the reaction rate.

Tidwell et al. were able to locate a TS and the zwitterion intermediate in the addition of trimethylamine to ketene at the HF/6-31+G* level, but no barrier or zwitterion intermediate
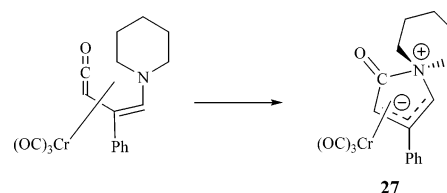


**Figure 7.** The crystalline nitrogen ylide isolated as the chromium−tricarbonyl complex.
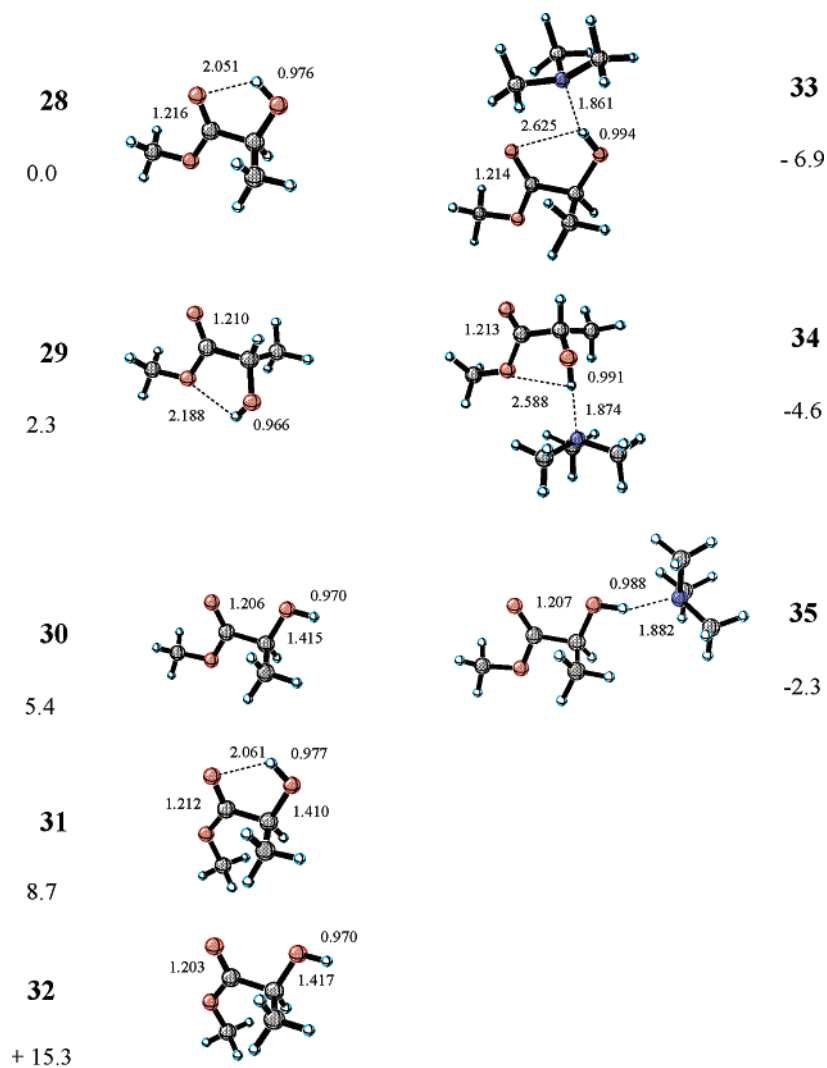
**Figure 8.** Conformers and relative energies of (*S*)-methyl lactate and trimethylamine complexes. Relative energies are in kcal/mol.

could be found at the MP2/6-31+G* level.[17] To our knowledge, only calculations carried out in a polar medium ($\epsilon = 40$) were successful in locating a stable equilibrium structure for the zwitterionic intermediate between pyridine[18] or trimethylamine[19] and the parent bisketene (carbon suboxide, $C_3O_2$).
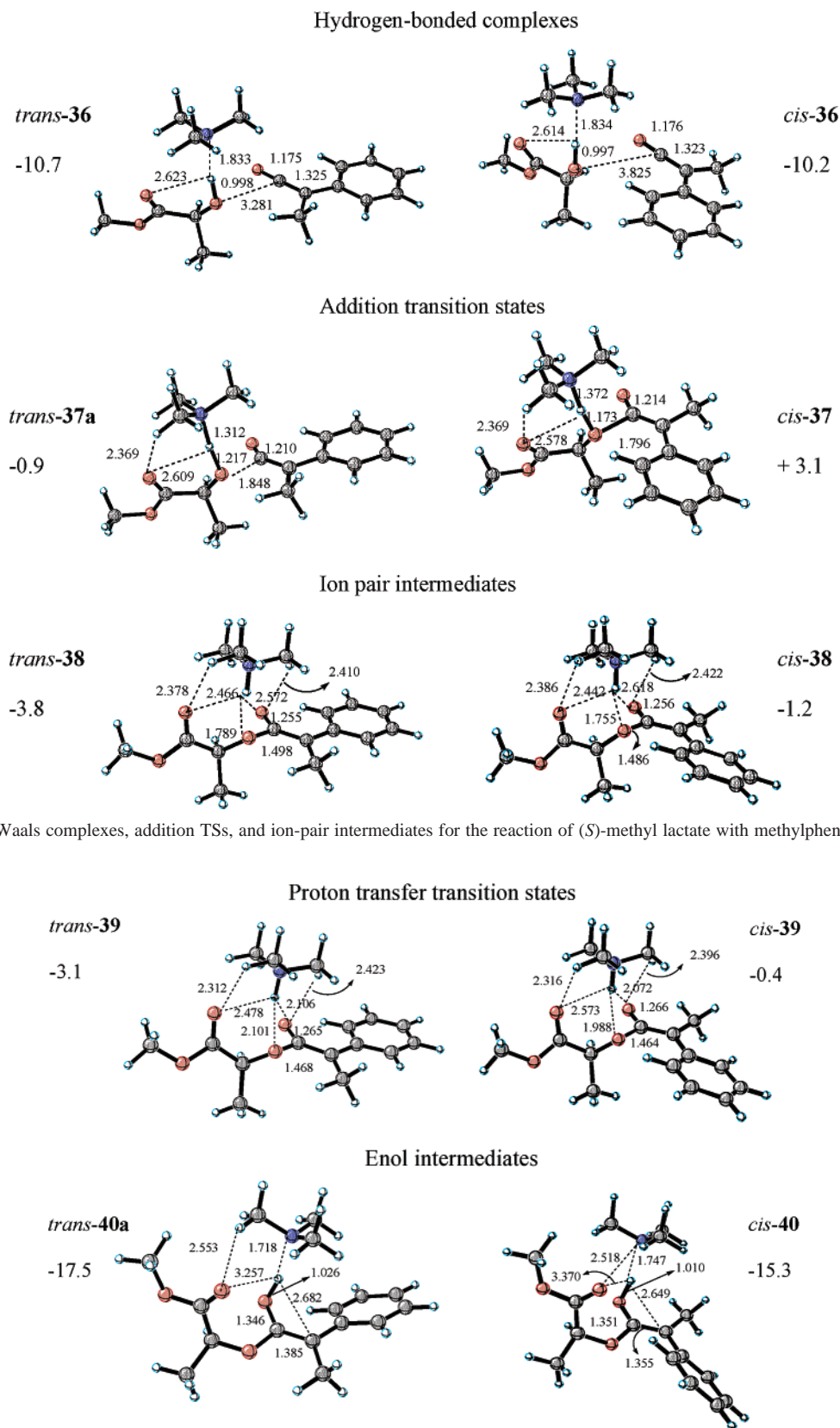
Direct observation of ylide adducts of ketenes and pyridine, **16−18**, has been achieved in solid argon matrixes (ca. 40 K) using FTIR spectroscopy, with ketenes such as dibenzopentafulvenone and derivatives,[20−22] **19−21**, dicarboalkoxyketenes,[23] **22−24**, dipivaloylketene,[24] and phenyl and 1-naphthylketenes,[24] **25** and **26**, shown in Figure 6. In these cases, where the negative charge can be efficiently stabilized by formation of an aromatic ring or by resonance delocalization onto an α-carbonyl group

or aromatic ring, ab initio calculations indicated that zwitterion formation is mildly exothermic and has a low activation energy in the gas phase.[23,25] So far, no ketene-trialkylamine ylides have been observed experimentally in argon matrices, and this suggests that the delocalization of positive charge in the pyridine ring is also important in stabilizing the corresponding zwitterions. To our knowledge, only one relevant nitrogen ylide, **27**, found from a trialkylamine, was isolated as the chromium-containing complex shown in Figure 7. Its structure was determined by X-ray diffraction.[26]

Recently, laser flash photolysis with time-resolved IR studies were carried out in acetonitrile ($\epsilon = 36.6$), to elucidate the mechanism and kinetics of the addition of various amines to a variety of ketenes.[27,28] An intermediate species identified as

(14) (a) Skancke, P. *J. Phys. Chem.* **1992**, *96*, 8065. (b) Duan, X.; Page, M. *J. Am. Chem. Soc.* **1995**, *117*, 5114. (c) Xie, J. F.; Yu, J. G.; Feng, W. L.; Liu, R. Z. *Theochem-J. Mol. Struct.* **1989**, *60*, 249−256. (d) Ruelle, P. *Chem. Phys.* **1986**, *110*, 273. (e) Nguyen, M. T.; Raspoet, G.; Vanquickenborne, L. G. *J. Phys. Org. Chem.* **2000**, *13*, 46−56. (f) Guthrie, J. P. *Can. J. Chem.* **1999**, *77*, 934−942. (g) Nguyen, M. T.; Raspoet, G. *Can. J. Chem.* **1999**, *77*, 817−829.
(15) Mackie, J. C.; Doolan, K. R. *Int. J. Chem. Kinet.* **1984**, *16*, 525−541.
(16) Curtiss, L. A.; Raghavachari, K.; Trucks, G. W.; Pople, J. A. *J. Chem. Phys.* **1991**, *94*, 7221.
(17) Raspoet, G.; Nguyen, M. T.; Kelly, S.; Hegarty, A. F. *J. Org. Chem.* **1998**, *63*, 9669−9677.
(18) Sung, K.; Tidwell, T. T. *J. Am. Chem. Soc.* **1998**, *120*, 3043−3048.
(19) Couturier-Tamburelli, I.; Aycard, J.-P.; Wong, M. W.; Wentrup, C. *J. Phys. Chem. A* **2000**, *104*, 3466−3471.

(20) Sessouma, B.; Couturier-Tamburelli, I.; Monnier, M.; Wong, M. W.; Wemtrup, C.; Aycard, J. P. *J. Phys. Chem. A* **2002**, *106*, ASAP.
(21) Qiao, G. G.; Andraos, J.; Wentrup, C. *J. Am. Chem. Soc.* **1996**, *118*, 5634−5638.
(22) De Lucas, N. C.; Netto-Ferreira, J. C.; Andraos, J.; Lusztyk, J.; Wagner, B. D.; Scaiano, J. C. *Tetrahedron Lett.* **1997**, *38*, 5147−5150.
(23) Andraos, J. *J. Phys. Chem. A* **2000**, *104*, 1532−1543.
(24) Visser, P.; Zuhse, R.; Wong, M. W.; Wentrup, C. *J. Am. Chem. Soc.* **1996**, *118*, 12598−12602.
(25) Kollenz, G.; Holzer, S.; Kappe, C. O.; Dalvi, T. S.; Fabian, W. M. F.; Sterk, H.; Wong, M. W.; Wentrup, C. *Eur. J. Org. Chem.* **2001**, 1315−1322.
(26) Fang, D.-C.; Fu, X.-Y. *J. Mol. Struct.* **1998**, *455*, 59−68.

**Hydrogen-bonded complexes**



**Addition transition states**



**Ion pair intermediates**



**Figure 9.** Van der Waals complexes, addition TSs, and ion-pair intermediates for the reaction of (*S*)-methyl lactate with methylphenylketene catalyzed by trimethylamine.

**Proton transfer transition states**



**Enol intermediates**



**Figure 10.** Proton transfer TSs and enol intermediates for the reaction of (*S*)-methyl lactate with methylphenylketene catalyzed by trimethylamine (energies in kcal/mol).

either zwitterionic ylide or amide enol formed in the nucleophilic addition of secondary amines to the $C_\alpha$ of the ketene. The kinetic data showed a much lower reactivity of tertiary amines (pyridine and triethylamine) as compared to secondary amines. The

observed trend was rationalized in terms of the steric effects exerted by both amine and ketene substituents.

Previous experimental and theoretical observations, and the experimental conditions and kinetics of the Merck process, seem
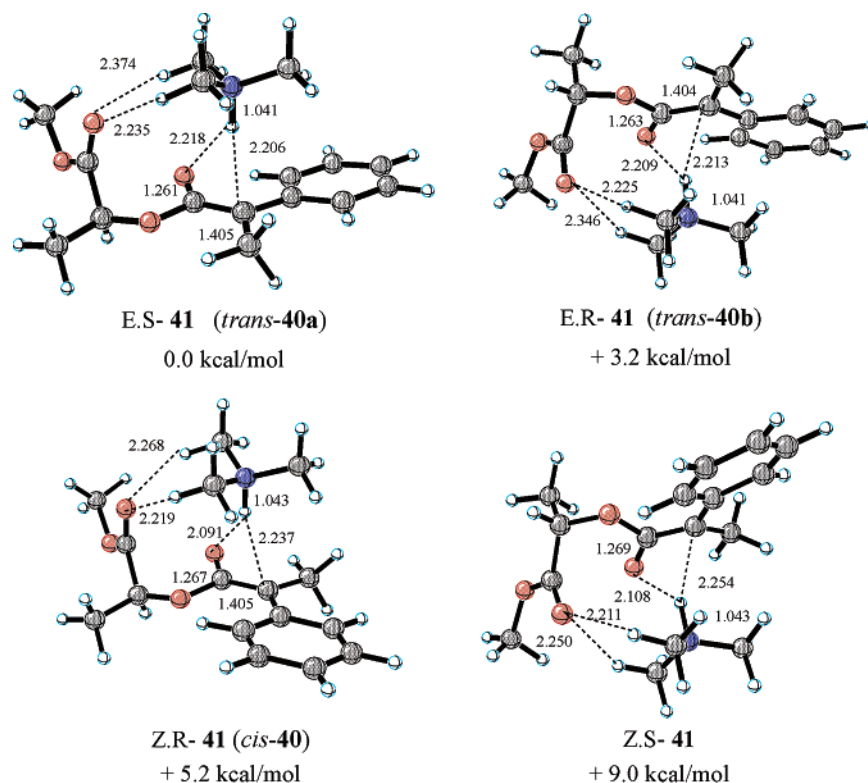
**Figure 11.** Tautomerization transition states for (*S*)-methyl lactate/methylphenylketene adducts. Relative energies are in kcal/mol. The intermediate enols that give rise to the corresponding tautomerization TSs are indicated in parentheses.

to favor alcohol addition to form either a zwitterion or an enol, followed by protonation or tautomerization to the ester product, when trimethylamine is used as the catalyst. This process would resemble the mechanism shown in Figure 4b postulated by Pracejus. We believe this mechanism is the more likely to operate with hindered tertiary bases in the gas phase and in nonpolar solvents. We expect the addition of trimethylamine to methylphenyl ketene to give the zwitterionic intermediate to become a competitive step only in polar solvents, therefore decreasing the diastereoselectivity of the Merck process as observed experimentally.

The Merck reaction was found to give maximum stereoselectivity at −78 °C in hydrocarbon solvents. It is first order in ketene, amine, and chiral alcohol, with a $k_H/k_D \gg 4$ for deuterated alcohols.[2a] We have explored variations on the mechanism theoretically for the reaction of (*S*)-methyl lactate with methylphenylketene, catalyzed by trimethylamine in the gas phase (90% dr; 87% ee after hydrolysis). The conditions are not too different from the experimental conditions, where the reaction is carried out in toluene solvent ($\epsilon = 2.38$). Calculations were also performed with two other chiral alcohols that show extreme values of selectivity, (*S*)-pantolactone (>98% dr; 99% ee), and (*S*)-3-methyl-2-butanol (8% ee), to provide a more detailed understanding of the factors responsible for diastereoselection. We carried out the calculations on (*S*)-pantolactone, even though the experiments were done with (*R*), so that the illustrations from computations could all be compared.
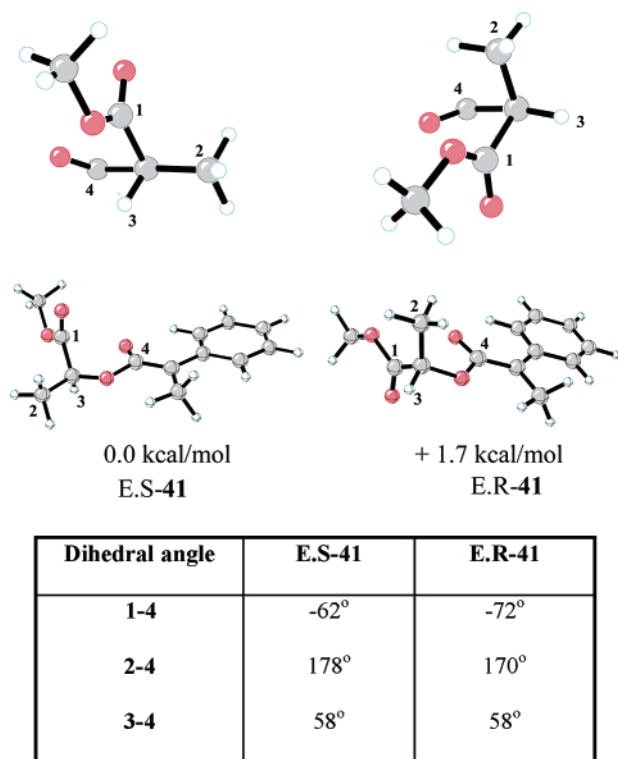
### Methodology

All stationary points were optimized and characterized by frequency analysis at the B3LYP[29]/6-31G* level using Gaussian 98.[30] The reported energies include zero-point energy corrections scaled by 0.9804.[31] All

transition states were further characterized by analysis of the normal modes corresponding to their imaginary frequencies and, in the case of the addition transition state, by intrinsic reaction coordinate (IRC) calculations.

### Results and Discussion

We first studied the conformational preferences of (*S*)-methyl lactate. Five different structures, **28**–**32**, were optimized and are shown in Figure 8. The most stable conformer **28** prefers the *s-cis* conformation around the O−C bond as in esters in general, to reduce the electronic repulsion between the lone pairs of electrons on the oxygen atoms. The alcohol hydroxyl is hydrogen-bonded to the carbonyl, forming a five-membered ring. Formation of an intramolecular hydrogen bond with the alkoxide oxygen gives conformer **29**, destabilized by 2.3 kcal/mol with respect to **28**. Disruption of the hydrogen bond in **28** results in the planar zigzag conformer **30**, destabilized by 5.4 kcal/mol with respect to **28**. Rotation around the O−C bond of

(27) Chelain, E.; Goumont, R.; Hamon, L.; Parlier, A.; Rudler, M.; Rudler, H.; Daran, J.-C.; Vaissermann, J. *J. Am. Chem. Soc.* **1992**, *114*, 8088−8098.
(28) Wagner, B. D.; Arnold, B. R.; Brown, G. S.; Lusztyk, J. *J. Am. Chem. Soc.* **1998**, *120*, 1827−1834.
(29) De Lucas, N. C.; Netto-Ferreira, J. C.; Andraos, J.; Scaiano, J. C. *J. Org. Chem.* **2001**, *66*, 5016−5021.
(30) (a) Lee, C.; Yang, W.; Parr, R. G. *Phys. Rev. B* **1988**, *37*, 785. (b) Becke, A. D. *J. Chem. Phys.* **1993**, *98*, 5648.
(31) Frisch, M. J.; Trucks, G. W.; Schlegel, H. B.; Scuseria, G. E.; Robb, M. A.; Cheeseman, J. R.; Zakrzewski, V. G.; Montgomery, J. A., Jr.; Stratmann, R. E.; Burant, J. C.; Dapprich, S.; Millam, J. M.; Daniels, A. D.; Kudin, K. N.; Strain, M. C.; Farkas, O.; Tomasi, J.; Barone, V.; Cossi, M.; Cammi, R.; Mennucci, B.; Pomelli, C.; Adamo, C.; Clifford, S.; Ochterski, J.; Petersson, G. A.; Ayala, P. Y.; Cui, Q.; Morokuma, K.; Malick, D. K.; Rabuck, A. D.; Raghavachari, K.; Foresman, J. B.; Cioslowski, J.; Ortiz, J. V.; Stefanov, B. B.; Liu, G.; Liashenko, A.; Piskorz, P.; Komaromi, I.; Gomperts, R.; Martin, R. L.; Fox, D. J.; Keith, T.; Al-Laham, M. A.; Peng, C. Y.; Nanayakkara, A.; Gonzalez, C.; Challacombe, M.; Gill, P. M. W.; Johnson, B.; Chen, W.; Wong, M. W.; Andres, J. L.; Gonzalez, C.; Head-Gordon, M.; Replogle, E. S.; Pople, J. A. *Gaussian 98*, revision A.7; Gaussian, Inc.: Pittsburgh, PA, 1998.

**0.0 kcal/mol**
**E.S-41**

**+ 1.7 kcal/mol**
**E.R-41**

| Dihedral angle | E.S-41 | E.R-41 |
|:---:|:---:|:---:|
| 1–4 | −62° | −72° |
| 2–4 | 178° | 170° |
| 3–4 | 58° | 58° |

***Figure 12.*** Dihedral angles in the tautomerization TSs for (*S*)-methyl lactate. Relative energies are in kcal/mol.

the ester group, while maintaining the intramolecular hydrogen bond to the carbonyl, gives the *s-trans* conformer **31**. Breakage of the hydrogen bond in **31** gives the least stable conformer **32**. These last two conformers **31** and **32** are greatly destabilized with respect to **28** (+8.7 and +15.3 kcal/mol, respectively) and were not further considered.

Complexes of trimethylamine, **33**–**35**, with conformers **28**, **29**, and **30** were studied. Conformers **28** and **29** are stabilized by 6.9 kcal/mol upon complex formation to give **33** and **34**, respectively. Although conformer **30** is more greatly stabilized (7.8 kcal/mol) by complex formation to give **35**, **33** remains the most stable conformer even after complexation and is probably the major conformer in nonpolar solvents.

Complex **33** can approach methylphenylketene either trans or cis to the phenyl group. Figure 9 shows the structures, *trans*-**36** and *cis*-**36**, and the relative energies of the van der Waals complexes resulting from electrostatic interaction between the hydroxyl oxygen and the ketene carbonyl carbon. The trans approach is favored by 0.5 kcal/mol and places the hydroxyl oxygen at 3.281 Å from the ketene carbonyl carbon, much closer than in the cis ternary complex (3.825 Å). Both termolecular complexes are stabilized by an additional 7 kcal/mol with respect to **33**.

From *trans*-**36** and *cis*-**36**, we found the corresponding addition transition states, *trans*-**37** and *cis*-**37**, by methodically decreasing the distance between the hydroxyl oxygen and the ketene carbonyl carbon. The addition transition states, *trans*-**37** and *cis*-**37**, are 9.8 and 13.3 kcal/mol above the corresponding termolecular complexes.

The transition states involve nucleophilic addition to the ketene carbonyl, assisted by deprotonation of the alcohol by trimethylamine. The addition occurs in the plane of the ketene substituents and is 4.0 kcal/mol lower for approach cis to the

methyl than for attack cis to the phenyl group. The phenyl group is nearly planar and presents substantial steric hindrance to attack. Transition state *trans*-**37a** is an earlier transition state with respect to the forming O–C bond (1.848 Å), which is much longer than in *cis*-**37** (1.796 Å), and also with respect to the elongation of the ketene carbonyl bond length. In the favored trans approach, trimethylamine is able to more efficiently increase the nucleophilicity of (*S*)-methyl lactate by forming a stronger hydrogen bond with the hydroxyl group, with the H–O bond 0.044 Å longer than that in the cis approach.

Intrinsic reaction coordinate (IRC) calculations on these addition transition states revealed that they connect the ternary complexes with the ion-pair intermediates, *trans*-**38** and *cis*-**38**, shown at the bottom of Figure 9. The unusual stability of these charge-separated species in the gas phase is likely due to the formation of three relatively strong hydrogen bonds between the $N^+$–H of the trimethylammonium and the three spatially close oxygen atoms, one from the ketene moiety (now bearing a formal negative charge) and two from the alcohol. Additional hydrogen bonds between the $N^+$–C–H bonds and the carbonyl oxygen further stabilize these ion pairs, with H⋯O distances ranging from 2.378 to 2.466 Å. The *trans*-**38** ion pair is 2.6 kcal/mol more stable than the *cis*-**38** probably due to the fact that *trans*-**38** shows a shorter $N^+$–H⋯O hydrogen bond to the enolate oxygen (2.572 versus 2.618 Å), and shorter $^+$N–CH---O bond lengths to the enolate oxygen (2.410 versus 2.422 Å), and to the carbonyl oxygen (2.378 versus 2.386 Å). The shortening of the O–C bond formed during the addition step brings the alkoxide in close proximity to the phenyl in *cis*-**38**, forcing the ring to rotate out of the plane of the enolate double bond by 14°.
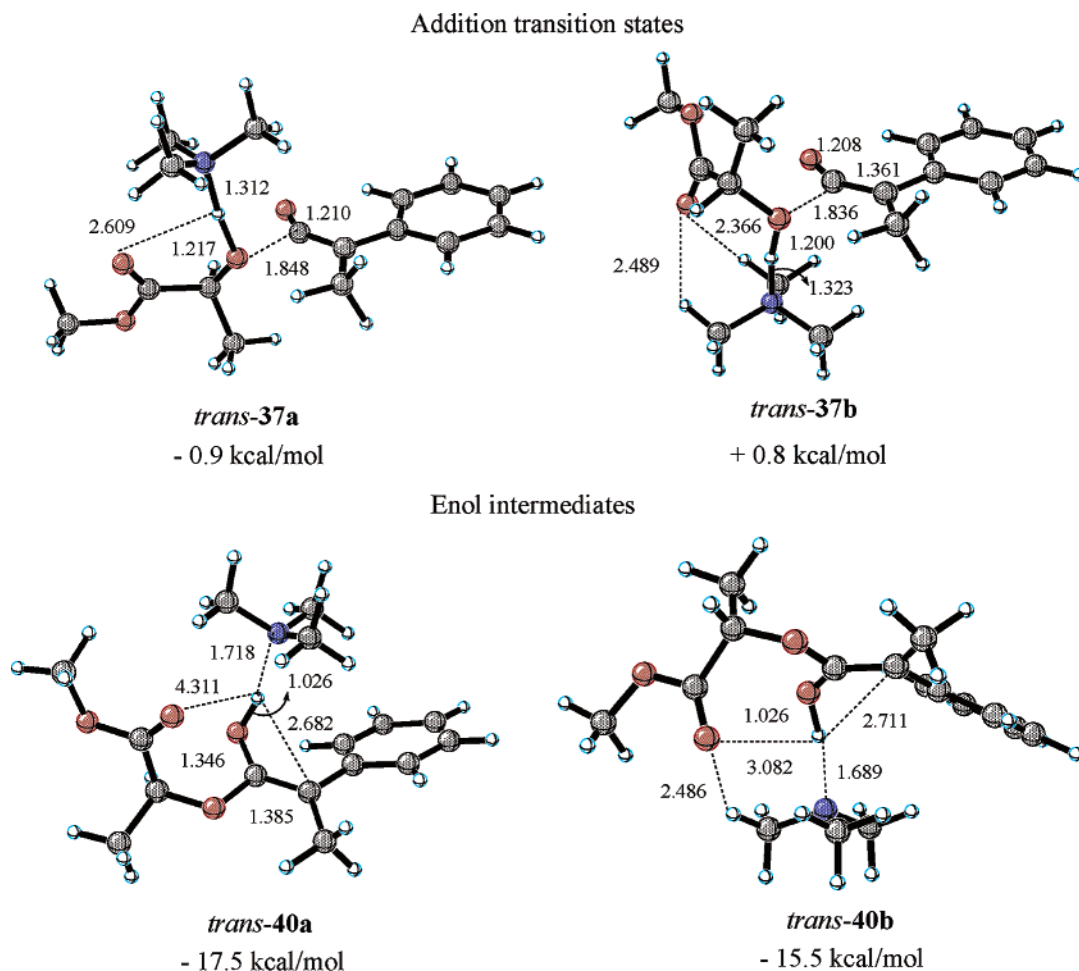
A second set of transition states, *trans*-**39** and *cis*-**39**, involve hydrogen transfer from the alkoxide oxygen to the enolate oxygen, which connects the ion pairs with the enols, *trans*-**40a** and *cis*-**40**. In both, the trimethylamine is hydrogen-bonded to the enolic OH (Figure 10). Transition state *trans*-**39** is only 0.7 kcal/mol above the ion-pair intermediate *trans*-**38** and is 2.7 kcal/mol more stable than transition state *cis*-**39**.

Transition state *trans*-**39** is later than *cis*-**39**, with the transferring proton equally distant (around 2.10 Å) from both oxygen atoms. The proton transfer is assisted by the (*S*)-methyl lactate carbonyl, which also remains hydrogen-bonded to the $N^+$–H (2.478 Å) and the $N^+$–C–H (2.312 and 2.519 Å) during the process.

The enol, *trans*-**40a**, is 2.2 kcal/mol more stable than *cis*-**40** due to a stronger N⋯HO hydrogen bond, as revealed by a shorter N⋯H distance (1.718 versus 1.747 Å) and longer H–O bond length (1.026 versus 1.010 Å), as well as lower steric hindrance of the nearly planar phenyl group.

The last step in the reaction involves the deprotonation of the enol and transfer of the proton to the carbon to form the ester product. The transition states calculated for this process resemble ion pairs of the trimethylammonium ion poised above the enolate anion. There are four such transition states shown in Figure 11: **E.S-41**, **E.R-41**, **Z.R-41**, and **Z.S-41**, where the first letter specifies the stereochemistry around the enol double bond and the second letter specifies the absolute chemistry of the newly created stereocenter. The lower energy enol *trans*-**40a**, formed from attack of the alcohol trans to the phenyl substituent, can have proton transfer along the top of the enolate,

## Addition transition states



*trans*-**37a**
− 0.9 kcal/mol

*trans*-**37b**
+ 0.8 kcal/mol

## Enol intermediates



*trans*-**40a**
− 17.5 kcal/mol

*trans*-**40b**
− 15.5 kcal/mol

**Figure 13.** Addition TSs and enol intermediates formed from (*S*)-methyl lactate and methylphenylketene. Structures are drawn with the new bond forming on the front side of the ketene, cis to the methyl. Structures on the left have the amine and lactate carbonyl above the ketene; those on the right have these functions below the ketene. Relative energies are in kcal/mol.

via transition state **E.S**-**41**, to form the (*S*,*S*) ester, or along the bottom of the enolate, via transition state **E.R**-**41**, to form the (*S*,*R*) ester. The former is 3.2 kcal/mol lower in energy. The remaining two transition states, **Z.R**-**41** and **Z.S**-**41**, involve *cis*-related lactate and phenyl groups. Once again, proton transfer along the top of the enolate, **Z.R**-**41**, is preferred (by 3.8 kcal/mol), now to give the (*S*,*R*) ester, but these two transition states are considerably higher in energy due to phenyl−lactate repulsion.

The key to the lower energy of **E.S**-**41**, and therefore to the stereoselectivity, is the lower energy of the lactate trans to phenyl, and the electrostatic attraction between the lactate carbonyl and the trimethylammonium ion. Figure 11 shows the distance from the carbonyl-O to the trimethylammonium C−H's. Stabilization arises from electrostatic interaction of the whole trimethylammonium group, which bears the positive charge, with the C=O dipole. The shortest distance from the carbonyl-O to a methyl-H is only 2.2 Å.

The stabilizing interaction is an example of the C−H···O= C hydrogen bond.[32] We have recently shown that the stabilizing interaction between trimethylammonium cation and methyl acetate, in the orientation shown in the transition state **E.S**-**41**, is worth 8.7 kcal/mol in the gas phase and 1.6 kcal/mol in

toluene.[33] For proton transfer to occur along the bottom face of the enolate, either this stabilization must be sacrificed, or the lactate must rotate into the unfavorable conformation shown in the transition state **E.R**-**41**, on the top right of Figure 11. This conformation suffers from repulsion between the α-methyl group of the lactate and the enolate oxygen, which is reflected in distorted dihedral angles around the *C−O bond. We optimized the structures of the enolates **E.S**-**41** and **E.R**-**41** obtained upon removal of the trimethylammonium cation from the corresponding transition states to estimate the conformational contribution to the stability of transition state **E.S**-**41.** Figure 12 shows the Fisher projections along the *C−O bond of the lactate moiety from the lower energy transition states **E.S**-**41** and **E.R**-**41**.

Enolate-**E.S**-**41** dihedral angles are −62°, 178°, and 58°, very close to a perfect staggered arrangement. In the less favorable enolate-**E.R**-**41**, on the other hand, the repulsion between the α-methyl group of the lactate and the enolate oxygen forces the methyl group (position 2) to move away, increasing its dihedral angle from the optimal −60° to −72°. Consequently, the hydrogen (position 3) dihedral angle changes to 170°, 10° away from the optimal anti arrangement. The lowest energy conformer, enolate-**E.S**-**41**, is 1.7 kcal/mol more stable than

(32) Wong, M. W. *Chem. Phys. Lett.* **1996**, *256*, 391−399.

(33) Vargas, R.; Garza, J.; Dixon, D. A.; Hay, B. P. *J. Am. Chem. Soc.* **2000**, *122*, 4750−4755.
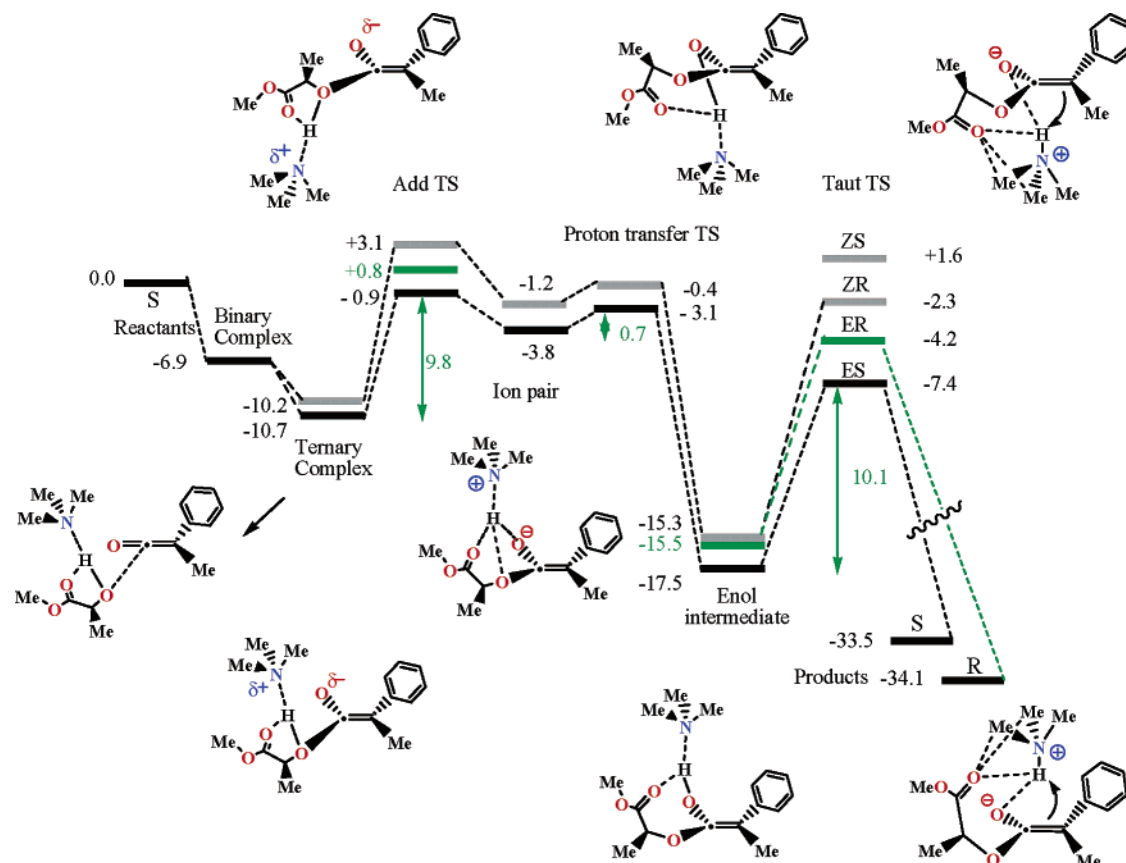
**Figure 14.** The relative energies, in kcal/mol, of reactants, intermediates, and transition states for (*S*)-methyl lactate.

enolate-**E.R**-**41** that places the enolate oxygen (position 4) between the two most sterically demanding substituents, the methyl (position 2) and the methyl ester (position 1) groups. Trimethylammonium increases this energy difference by fixing these conformations with hydrogen bonds.

The second best tautomerization transition state **E.R**-**41** also arises from the enol that has the hydroxyl group trans to the phenyl. Now the carbonyl of the lactate and the trimethylamonium ion are below the plane of the ketene. Enol *trans*-**40b**, the precursor of TS **E.R**-**41**, could be formed by addition of the alcohol via the addition transition state *trans*-**37b**, or by a conformational change of the most stable enol, *trans*-**40a**, that most likely involves decomplexation of trimethylamine followed by rotation around the *C–O bond of the lactate moiety. Figure 13 shows the transition states for the addition of (*S*)-methyl lactate with the amine and carbonyl above or below the plane. The addition transition state *trans*-**37b** is 1.7 kcal/mol higher in energy than *trans*-**37a**, while enol *trans*-**40a** is 2.0 kcal/mol more stable than enol *trans*-**40b**.

If the rotational barrier to convert *trans*-**40a** into *trans*-**40b** is lower than 10.1 kcal/mol, the $E_a$ for the tautomerization of enol *trans*-**40a** to the ester product, the enols will be in equilibrium and the stereoselectivity of the whole process will be determined during the last tautomerization step. If, on the other hand, the isomerization of enols requires more than 10 kcal/mol, the stereoselectivity will be determined in the addition step.

Starting from enol *trans*-**40a**, there are two rotational barriers that correspond to the carbonyl of the lactate rotating toward

or away from the enol oxygen. These barriers were estimated to be 3.9 and 10 kcal/mol, respectively, by sequentially changing the dihedral angle around the *C–O bond in the hydrogen-bonded complex *trans*-**40a**, and optimizing the rest of structure. These results suggest that enols *trans*-**40a** and *trans*-**40b** are in equilibrium, and that the diastereoselectivity will be determined in the last tautomerization step.

The relative energies of reactants, intermediates, and transition states along the lowest energy pathway are shown in Figure 14. The stereoisomeric transition states and intermediates corresponding to an approach of the alcohol cis to the phenyl in the ketene are not shown, but their higher energies are represented in the figure by gray horizontal bars. The stereoisomeric addition transition state and enol intermediate corresponding to an approach of the alcohol trans to the phenyl in the ketene, but where the carbonyl of (*S*)-methyl lactate is facing below the plane of the ketene, are shown above the diagram, and their higher energies are represented in the figure by green horizontal bars. The energetics are consistent with a kinetically controlled process, and the major product is the higher energy (*S*)-diastereomer.

In the postulated mechanistic scheme, which constitutes a case of the "conducted tour mechanism" postulated by Cram,[34] the hydrogen originally present in the alcohol becomes alternatively hydrogen-bonded or even covalently bonded to different nitrogen or oxygen atoms to form transition states and inter-

(34) Cannizzaro, C. E.; Houk, K. N. *J. Am. Chem. Soc.* **2002**, *124*, 7163–7169.
(35) Cram, D. J. *Fundamentals of Carbanion Chemistry*; Academic Press: New York, 1965; Chapter III, p 101.
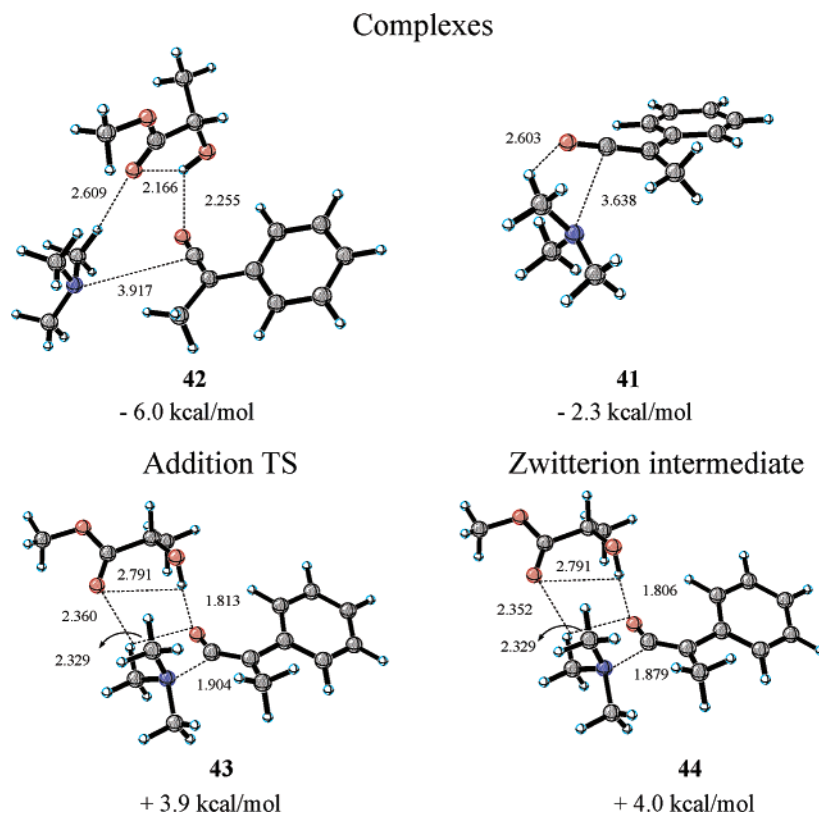
Complexes



**42**

- 6.0 kcal/mol

**41**

- 2.3 kcal/mol

Addition TS

Zwitterion intermediate

**43**

+ 3.9 kcal/mol

**44**

+ 4.0 kcal/mol

**Figure 15.** Addition of trimethylamine to methylphenylketene assisted by (*S*)-methyl lactate. Relative energies are in kcal/mol.
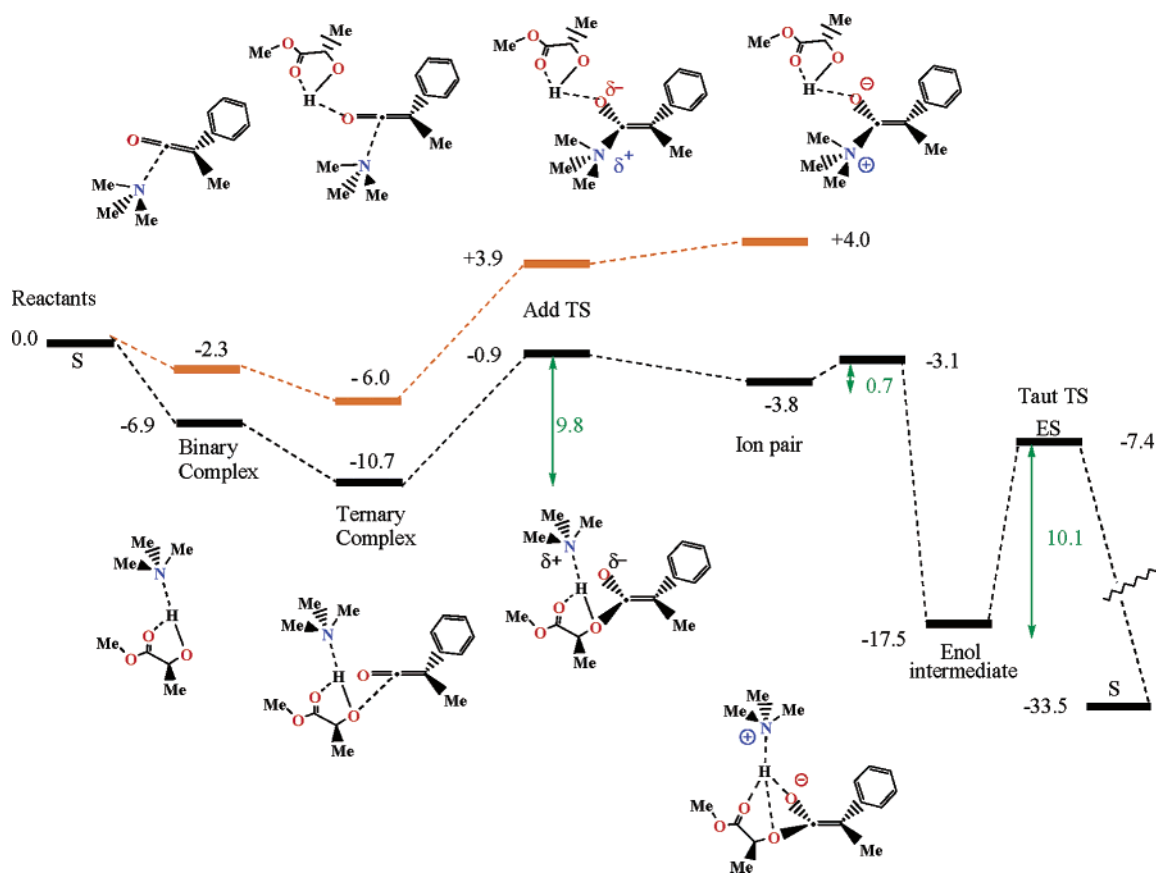


**Figure 16.** The relative energies (kcal/mol) of reactants, intermediates, and transition states along the lowest energy pathways of the amine (orange) and alcohol (black) addition reactions.

mediates. Throughout this process, trimethylamine takes the alcohol hydrogen on a "conducted tour" along one face of the

substrate (or along both faces upon equilibration or rotamers *trans*-**40a** and *trans*-**40b**), from one hydrogen-bonding site to
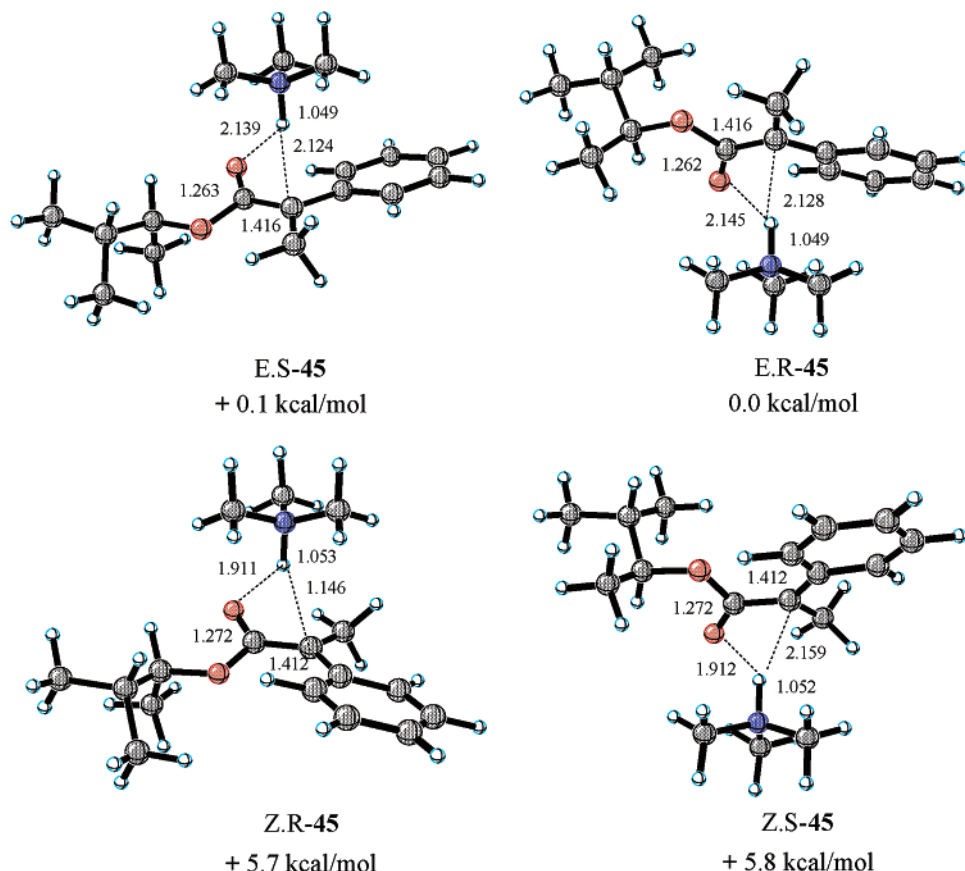
**Figure 17.** Tautomerization transition states for (*S*)-3-methyl-2-butanol. Relative energies are in kcal/mol.

the next without wandering out into the medium. Polar solvents "hijack" this atom, breaking up the ion pair and lowering the stereoselectivity as a result.

We have also explored an alternative nucleophile-catalyzed mechanism involving the addition of trimethylamine to methylphenylketene. The structure of a van der Waals complex between trimethylamine and methylphenylketene, **41**, is 2.3 kcal/mol more stable than the separated reactants, but still considerably higher in energy than any of the intermediates postulated earlier (Figure 15).

No barrier could be located for the addition of trimethylamine to methylphenyl ketene at the B3LYP/6-31G* level, in agreement with previous results at the MP2/6-31+G*//HF/6-31+G* level for the addition of trimethylamine to ketene.[16] The zwitterion is not a stable species in the gas phase.

When (*S*)-methyl lactate is hydrogen-bonded to the ketene carbonyl, the complex of ketene and trimethylamine is stabilized by an additional 3.7 kcal/mol, **42**. A transition state was found for the addition of trimethylamine to the ketene, **43**, assisted by an alcohol molecule. The zwitterionic product, **44**, is structurally very similar to the transition state and is 0.1 kcal/mol higher in energy. Figure 15 shows the fully optimized structures. From this zwitterion, proton transfer to form either the enol or the ester is unfavorable in the gas phase.

The relative energies of reactants, intermediates, and transition states along the lowest energy pathway for the addition of (*S*)-methyl lactate to ketene catalyzed by trimethylamine are represented in Figure 16 by black horizontal bars. The relative energies of reactants, complexes, the addition transition state, and ion-pair intermediate for the addition of trimethylamine to

ketene assisted by (*S*)-methyl lactate are shown in the same figure with orange horizontal bars. The transition state for the addition of (*S*)-methyl lactate to ketene catalyzed by trimethylamine is 4.8 kcal/mol more stable that the transition state for the addition of trimethylamine to ketene assisted by (*S*)-methyl lactate. The alcohol addition is clearly the preferred reaction pathway.

From the energy profile of the preferred mechanism shown in Figure 14, it is evident that the alcohol addition step is rate determining and should give rise to the observed kinetic isotope effect, while the enol−keto tautomerization is the step that determines the stereochemistry of protonation at carbon.

The kinetic isotope effect for addition of lactate OH versus OD was calculated from zero-point energy differences based on the Eyring transition state theory. We obtained a $k_H/k_D = 4.1$ at 25 °C. This corresponds to $k_H/k_D = 8.3$ at −78 °C. The calculated value at −78 °C is much higher than the experimental value of 4 found for the addition of (*S*)-ethyl lactate. Hydrogen tunneling is known to be usual for proton transfer, although this would have been expected to make the KIE larger experimentally.

The theoretical exploration of lactate addition to methylphenylketene provides a satisfying picture of the origin of stereoselectivity; the preferred conformation of the lactate moiety in the intermediate steers the protonation in the sense found experimentally. To establish the validity of the explanation, we have also explored the addition of (*S*)-3-methyl-2-butanol, which adds experimentally with no significant selectivity, and also of pantolactone, the addition of which proceeds with the highest observed stereoselectivity. The latter provided a surprise, and
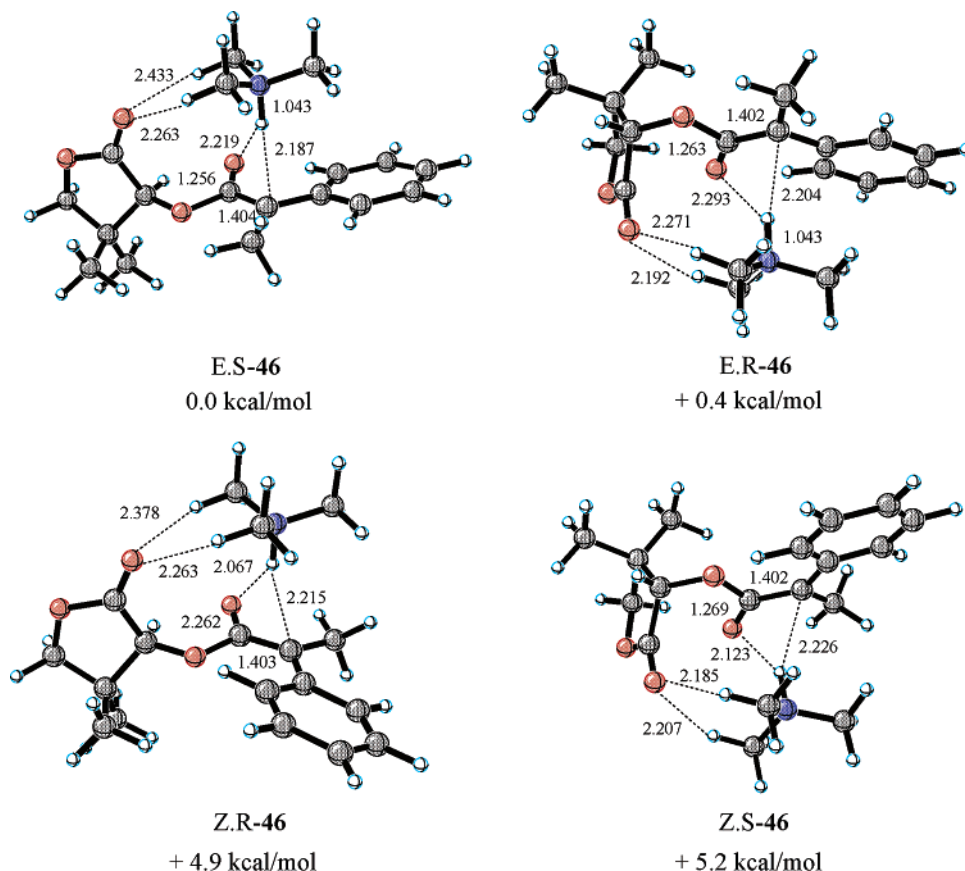
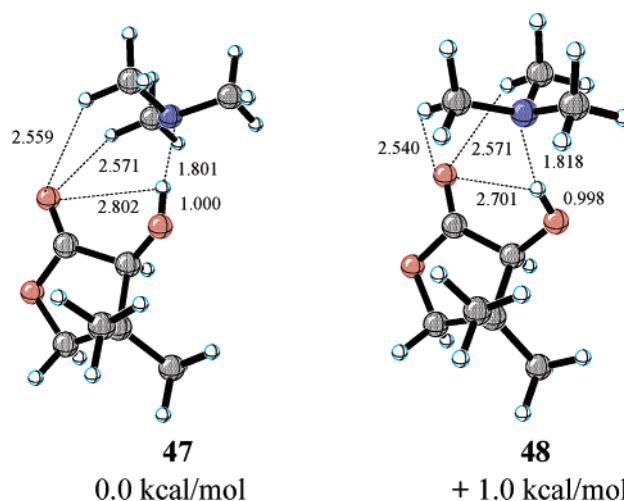**Figure 18.** Tautomerization transition states for (*S*)-pantolactone. Relative energies are in kcal/mol.

also some additional insights into how the stereoselectivity develops in the reactions.

The reactions of (*S*)-3-methyl-2-butanol are found experimentally to be unselective, proceeding in a 46:54 ratio favoring slightly the (*R*)-configuration at the new stereocenter, corresponding to 8% ee. The most selective chiral alcohol, (*S*)-pantolactone, exhibits an enantiomeric ratio of 99.5:0.5 in favor of the (*S*)-configuration at the newly created chiral carbon, corresponding to 99% ee in the formation of the final acid product.

The model described here predicts that the α-carbonyl group is required to steer the enolate protonation in a stereoselective fashion. The carbonyl determines the relative energies of the enol–keto tautomerization transition states. The absence of this hydrogen-bond acceptor group at the stereogenic position should decrease the stereoselectivity. The model also predicts that a bulkier alkyl substituent (e.g., the dimethyl group of pantolactone, the last entry in Scheme 1) at the stereogenic center should increase the stereoselectivity. This more sterically demanding alcohol would increase the energies of transition states for proton transfer "below" the enolate plane, by forcing the quaternary center into the crowded region near the carbonyl group.

As expected, calculations with (*S*)-3-methyl-2-butanol predict that the selectivity is very low. The tautomerization transition state **E.R**-**45** is now 0.1 kcal/mol more stable than **E.S**-**45**, and the other two transition states, **Z.R**-**45** and **Z.S**-**45**, are much higher in energy (Figure 17). No significant stereoselectivity is predicted, as found experimentally.

The (*S*)-pantolactone calculations are summarized in Figure 18. Surprisingly, in contrast to experiment, the relative energies
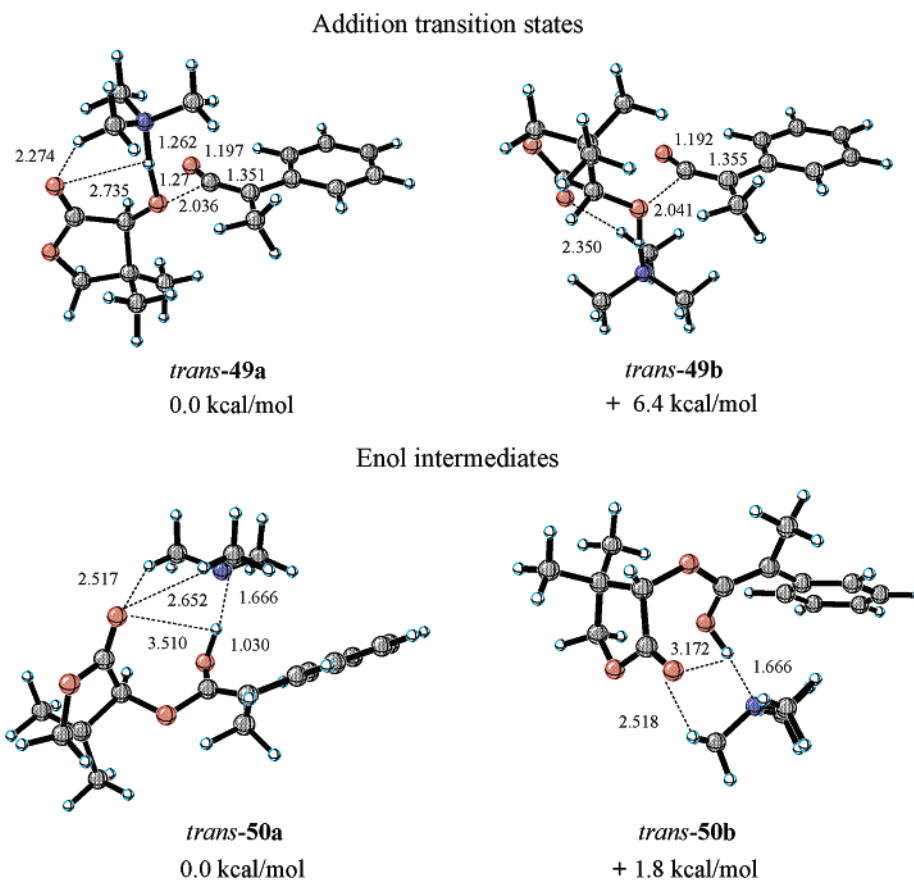


**47**
0.0 kcal/mol

**48**
+ 1.0 kcal/mol

**Figure 19.** Conformers of (*S*)-pantolactone hydrogen-bonded to trimethylamine. Relative energies are in kcal/mol.
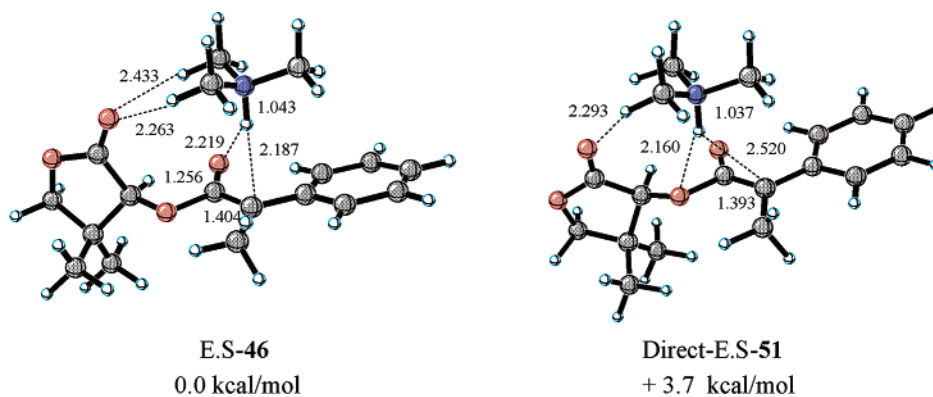
of the four tautomerization transition states indicate that the selectivity should be greatly reduced when compared to those with (*S*)-methyl lactate. Transition state **E.S**-**46** is only 0.4 kcal/mol lower in energy than the **E.R**-**46**, and the other two transition states for protonation are much higher in energy.

While the tertiary carbon must be placed in the vicinity of the ester carbonyl oxygen in **E.R**-**46**, this turns out to cost only 0.4 kcal/mol, rather than the much higher difference that would be required to explain the high stereoselectivity of the pantolactone reaction.

The selectivity must therefore be determined in an earlier step. Consequently, the entire reaction pathway was explored.

Addition transition states



*trans*-**49a**
0.0 kcal/mol

*trans*-**49b**
+ 6.4 kcal/mol

Enol intermediates



*trans*-**50a**
0.0 kcal/mol

*trans*-**50b**
+ 1.8 kcal/mol

**Figure 20.** Addition transition states and enol intermediates for (*S*)-pantolactone. Relative energies are in kcal/mol.



E.S-**46**
0.0 kcal/mol

Direct-E.S-**51**
+ 3.7 kcal/mol

**Figure 21.** Comparison of protonation transition states for the tautomerization of (*S*)-pantolactone enolate. Relative energies are in kcal/mol.

Conformational studies on (*S*)-pantolactone hydrogen-bonded to trimethylamine gave two conformers, **47** and **48**, shown in Figure 19. Complex **47** is 1.0 kcal/mol more stable than **48** and has somewhat better N····H−O hydrogen bonding with trimethylamine tilted away from the gem-dimethyl group.

All of the previous calculations show that nucleophilic attack occurs preferentially trans to the phenyl group of the ketene, and so only these were computed for pantolactone. Transition states with the carbonyl group of (*S*)-pantolactone and the hydrogen-bonded trimethylamine above or below the plane of the ketene were located. These addition transition states, *trans*-**49a** and *trans*-**49b**, and the corresponding enol products of addition are shown in Figure 20. The increased steric hindrance at the chiral center, when compared to (*S*)-methyl lactate, significantly affects the relative energies of the addition transition states, making transition state *trans*-**49a** 6.4 kcal/mol lower

in energy than *trans*-**49b**. This significant energetic difference is due to steric hindrance and repulsive electrostatic interactions. In transition state *trans*-**49b**, the hydrogens of the gem-dimethyl group in the lactone ring are 2.59 Å away from the ketene oxygen, a distance shorter than the sum of their van der Waals radii (2.7 Å). In transition state *trans*-**49a**, on the other hand, the distance between those groups is larger, 3.33 Å.
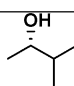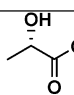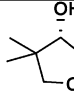
*Trans*-**49a** is also more stable because there is a weak hydrogen bond between the hydrogen at the chiral center and the ketene oxygen (2.26 Å) that is developing a negative charge. This stabilizing interaction is replaced by an electrostatic repulsion between the carbonyl oxygen of the pantolactone and the ketene oxygen in *trans*-**49b**.

The large difference in $E_a$ values found in the rate-limiting step ensures that the most stable enol intermediate, enol-**50a**, is formed exclusively. If the two enols, enol-**50a** and enol-**50b**,
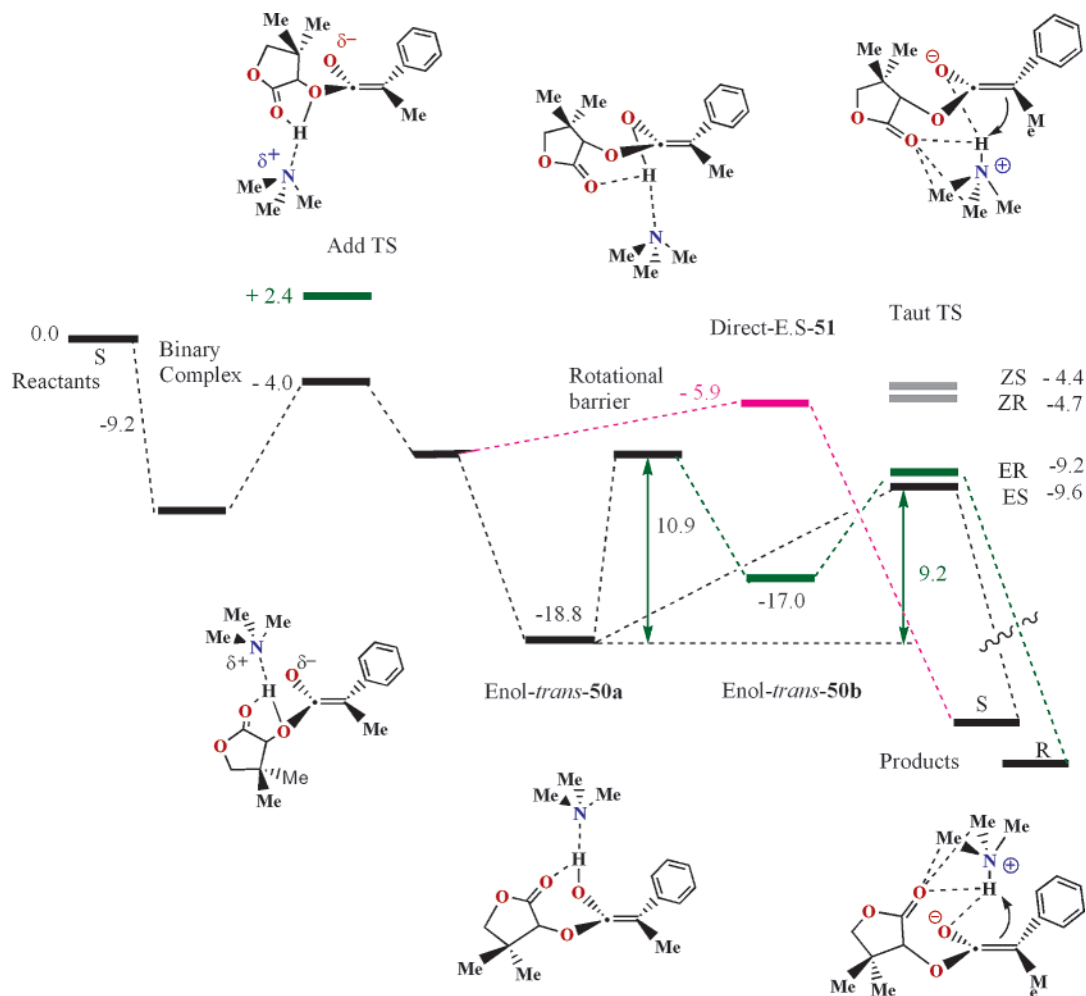
**Figure 22.** Energy profile for the reaction of (*S*)-pantolactone and methylphenylketene catalyzed by trimethylamine. Relative energies are in kcal/mol.

**Table 2.** Quantitative Comparison between Experimental and Calculated Selectivities

| (*S*)- ROH | Experimental d.r. (*S:R*) | Experimental $\Delta\Delta G^{\pm}$ d.r. | Experimental e.r. (*S:R*) | Experimental $\Delta\Delta G^{\pm}$ e.r. | Calculated $\Delta\Delta H^{\pm}$ |
|---|---|---|---|---|---|
| OH (isopropyl) | NA | NA | 46:54  8% ee | 0.1 kcal/mol | 0.1 kcal/mol  Tautomerization |
| OH ...O-Me, O (ester) | 95:5  90% d.r. | 1.1 kcal/mol | 93.5: 6.5  87% ee | 1.0 kcal/mol | 3.2 kcal/mol  Tautomerization |
| OH ...O, O (lactone) | > 99:1  > 98 % d.r. | >2.1 kcal/mol | 99.5:0.5  99% ee | >2.1 kcal/mol | 6.4 kcal/mol  Addition |

were able to interconvert easily, a mixture of both of these would be present at equilibrium, and the process would be nonselective due to the similar energies of the corresponding tautomerization transition states.

An approximate value for the rotational barrier that connects enol *trans*-**50a** and enol *trans*-**50b** was obtained by incrementally changing the dihedral angle around the *C—O bond of *trans*-**50a**, and optimizing the rest of the structure. We expect the rotational barriers estimated in this fashion to represent the lower limit to the energetic cost associated with the process

that involves not only rotation around the *C—O bond, but also decomplexation of the base, rotation of the enol OH, and final complexation of trimethylamine from the opposite face of the enolate plane. Two barriers of +13.5 and +10.9 kcal/mol connect the two conformers of the hydrogen-bonded complex. Starting from the most stable conformer *trans*-**47a**, the lowest energy barrier corresponds to rotation of the carbonyl of pantolactone toward the enolate oxygen; this barrier is 1.7 kcal/mol higher than the tautomerization activation barrier. Upon rotation in this direction, the steric hindrance increases to a
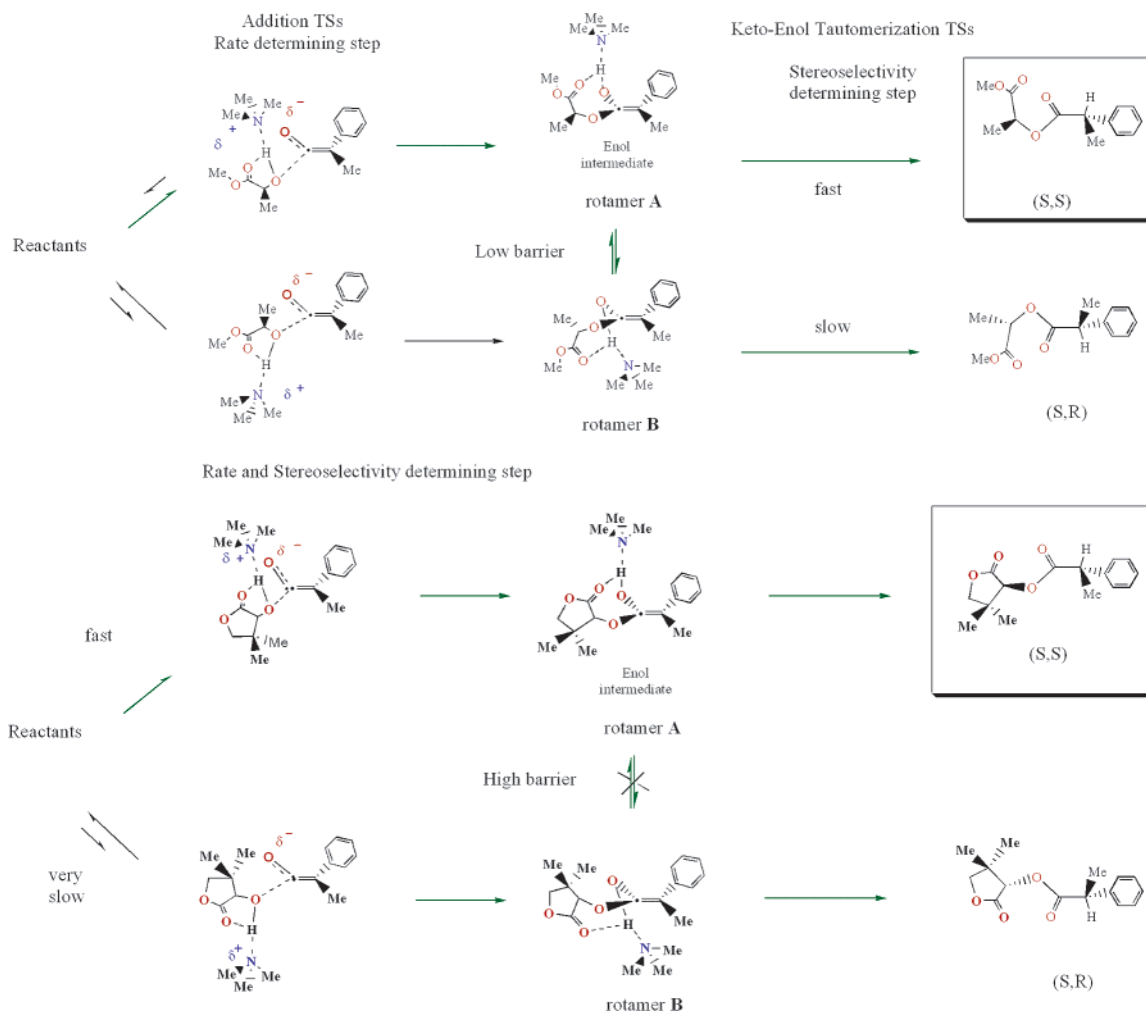
**Figure 23.** Summary of mechanisms of asymmetric additions of chiral alcohols to ketenes.

maximum when the carbonyl of pantolactone crosses the plane of the enol. Due to the conformational restriction of the pantolactone ring, the steric hindrance cannot be relieved, and this barrier is higher than the corresponding barrier of the intermediate enol formed from (*S*)-methyl lactate. These results indicate that, in the case of (*S*)-pantolactone, there is no enol equilibration; therefore, the diastereoselectivity is determined in the addition transition step.

We have also investigated the possibility of direct proton transfer from the ion-pair *trans*-**38** to the enolate carbon to give the product, via transition state Direct-**E.S**-**51**. Figure 21 shows a comparison between the lowest energy tautomerization TS, **E.S**-**46**, and the latter transition state Direct-**E.S**-**51**. The tautomerization transition state is 3.7 kcal/mol lower in energy than Direct-**E.S**-**51**, and therefore will prevail.

The relative energies of reactants, intermediates, and transition states along the lowest energy pathway are shown in Figure 22. The stereoisomeric tautomerization transition states corresponding to an approach of (*S*)-pantolactone cis to the phenyl in the ketene are not shown, but their higher energies are represented in the figure by gray horizontal bars. The stereoisomeric addition transition state and enol intermediate corresponding to an approach of the alcohol trans to the phenyl in the ketene, but where the carbonyl of (*S*)-pantolactone is facing below the ketene plane, are shown, and their higher energies

are represented by green horizontal bars. Direct-**E.S**-**51** is not shown, but its energy is represented by a pink horizontal bar.

The energy profile presented in Figure 22 shows that when the rotational barrier is higher than the $E_a$ of the tautomerization of enol *trans*-**50a** to product, enol *trans*-**50a** will tautomerize faster to product than equilibrate with enol *trans*-**50b**. Therefore, when (*S*)-pantolactone is used, the diastereoselectivity is determined during the addition transition state and maintained throughout the process due to the conformational constraints of the sterically demanding five-membered ring.

In the (*S*)-3-methyl-2-butanol case, the calculation of tautomerization TSs shows that diastereoselection is lost, supporting the proposed mechanism. Due to the absence of steering carbonyl, and therefore the formation of an extra hydrogen bond between the base and the approaching alcohol, the ROH---NMe₃ complex has greater conformation flexibility than either lactate or pantolactone. Therefore, we do not expect major energetic differences between the two lowest energy diastereoisomeric addition TSs in this case. Yet even if they were very different energetically, the rotational barriers for the corresponding enols would be low, and enol equilibration would most probably prevail, rendering the process nonselective.

Table 2 shows a quantitative comparison between experimental and calculated selectivities. The differences between diastereomeric and enantiomeric ratios are small in the lactate

and pantolactone cases. Although the calculated differences in activation enthalpies are larger than the experimentally determined differences in activation free energies, our mechanism accounts for the lack of selectivity of 3-methyl-2-butanol, the relatively higher selectivity of methyl lactate, and the highest selectivity of pantolactone. We believe that the overestimation of the free energy difference is most likely due to the fact that many conformers of the chiral alcohols and their corresponding hydrogen-bonded complexes with the base contribute to the reaction pathway described.

## Conclusion

The mechanisms predicted by the calculations account for the preferred stereoisomer in each reaction, the fact that stereoselectivity is only high in nonpolar solvents, and the special role of small trialkylamine bases. Polar solvents would disrupt the tight ion-pair transition state and decrease steering of the proton transfer along one face of the enolate by the lactate ester. Furthermore, polar solvents may induce a change of mechanism by stabilizing zwitterionic structures of type **9** (Figure 4) that correspond to an initial nucleophilic attack of the base on the ketene carbonyl. The trimethylammonium is ideal for carbonyl steering by C—H····O=C hydrogen bonding. The model also indicates why a medium-sized alkyl substituent at the stereogenic center (i.e., methyl group in (*S*)-methyl lactate) increases the stereoselectivity. This will increase the energies of transition states for proton transfer "below" the enolate plane,

by forcing the quaternary center into the crowded region near the carbonyl group. A more sterically demanding alkyl substituent at the stereogenic center (i.e., pantolactone) improves the steroselectivity in a different way, by increasing the energy of the addition transition state of the alcohol with the carbonyl group below the plane of the enolate. It also increases the barrier for the conformational equilibrium between the two enols (Figure 23).

The precise nature of the aryl group on the other hand is unimportant, because even a phenyl produces essentially one addition pathway, and additional bulk on the aryl group will mostly reside away from the area where nucleophilic attack occurs.

The model for the remarkable 1,4-asymmetric induction observed in these reactions uncovers new factors controlling stereoselectivity and provides a guide as to how stereoselective reactions might be achieved in other cases.

**Supporting Information Available:** Experimental details. This material is available free of charge via the Internet at http://pubs.acs.org.

JA035899+